AIP | Journal of Applied Physics

Core/shell magnetism in NiO nanoparticles

J. F. K. Cooper, A. Ionescu, R. M. Langford, K. R. A. Ziebeck, C. H. W. Barnes et al.

Citation: J. Appl. Phys. **114**, 083906 (2013); doi: 10.1063/1.4819807
View online: http://dx.doi.org/10.1063/1.4819807
View Table of Contents: http://jap.aip.org/resource/1/JAPIAU/v114/i8
Published by the AIP Publishing LLC.

Core/shell magnetism in NiO nanoparticles

J. F. K. Cooper,[1] A. Ionescu,[1] R. M. Langford,[1] K. R. A. Ziebeck,[1] C. H. W. Barnes,[1] R. Gruar,[2] C. Tighe,[2] J. A. Darr,[2] N. T. K. Thanh,[3,4] and B. Ouladdiaf[5]
[1]*TFM Group, Cavendish Laboratory, Cambridge University, JJ Thomson Ave., Cambridge CB3 OHE, United Kingdom*
[2]*Chemistry Department, University College London, 20 Gordon St., London WC1H 0AJ, United Kingdom*
[3]*Davy-Faraday Research Laboratory, Royal Institution of Great Britain, 21 Albemarle St., London W1S 4BS, United Kingdom*
[4]*Department of Physics and Astronomy, University College London, Gower Street, London WC1E 6BT, United Kingdom*
[5]*Institut Laue-Langevin, 6 Rue Jules Horowitz, 38042 Grenoble, France*

(Received 13 March 2013; accepted 15 August 2013; published online 28 August 2013)

The anomalous appearance of a ferromagnetic moment in nominally antiferromagnetic nanoparticles has been known about since Néel, but never well understood. We present proof of the core/shell model of magnetism in antiferromagnetic NiO nanoparticles (NP) using neutron diffraction. Nickel oxide nanoparticles were produced in a large quantity by a novel continuous hydrothermal flow synthesis method. The antiferromagnetic nature of the nanoparticles allowed the structural and the magnetic diffraction peaks to be completely separated. Using both the microstructure option in "Fullprof" microstructure fitting suite and convolution techniques, we determined the NP consisted of an ordered antiferromagnetic core 5.2(2) nm in diameter surrounded by a disordered shell 0.7(2) nm thick. Further magnetic measurements showed that this disordered shell possess a significant polarisable magnetisation, up to a fifth that of pure nickel. They also indicate that two magnetic transitions occur between 400 and 10 K; around 350 K, there is a broad transition from paramagnetic to a form of superparamagnetism, then near 30 K there is a transition to a higher anisotropy state. Differences in field cooled and zero field cooled hysteresis loops were found, though with no evidence of exchange bias effects. © *2013 AIP Publishing LLC*. [http://dx.doi.org/10.1063/1.4819807]

INTRODUCTION

Recently, magnetic nanoparticles (MNPs) have become a subject of intense research in a myriad of different fields, from catalysis[1,2] and pattern formation[3] to MRI contrast agents[4] and for diagnoses in magnetic biosensors.[5] One of the most studied areas of research is biomedical and clinical applications of MNP,[6,7] either as a means of targeted drug delivery[8,9] or for magnetic hyperthermia to treat cancer.[10–12] Many of these applications require control over the magnetic properties of the particles, which has so far lagged behind the advanced research into the various growth techniques of MNP.[8]

A feature common to both superparamagnetic and ferromagnetic MNPs is the addition of correction factors, which must be included when calculating their magnetisation compared to the expected bulk value. These factors are predominantly explained as accounting for finite size effects; however, the nature of these effects is as yet, unresolved. Many have conjectured that it is a surface anisotropy, which causes these surface spins to become non-magnetic or orientate in a different configuration from the core spins.[13,14]

There has been a plethora of recent work on the magnetic properties of antiferromagnetic nanoparticles, many of which report the well known existence of a ferromagnetic moment on the NP.[15–18] A common theory put forward to explain this ferromagnetic enhancement is a form of core/shell model where the core spins are antiferromagnetically aligned and the outer shell spins somehow give rise to the ferromagnetic moment.[16,17,19] It is mathematically proven that systems such as these must exhibit frustration at the surface;[20] however, there is currently no agreement as to the exact nature of the shell and the cause of the moment.

This work aims to unambiguously show the existence of the magnetically disordered outer layer and the validity of the "core/shell" model in single crystal magnetic NP. We approach this with a combination of neutron powder diffraction and magnetometry measurements. Using neutron diffraction allows the NP magnetism to be probed simultaneously with the structural information, which could otherwise be obtained by conventional x-ray diffraction. In order to completely separate the magnetic from the structural diffraction peaks, we used uncoated antiferromagnetic NiO nanoparticles.

EXPERIMENTAL

NiO has a simple NaCl structure with the space group $Fm\bar{3}m$ and a lattice parameter of $a = 4.168(6)$ Å. Below the Néel temperature ($T_N = 523$ K), NiO orders antiferromagnetically with a [½ ½ ½] propagation vector producing a type 2 *fcc* structure in which the moments in {1 1 1} planes are coupled ferromagnetically, while in the adjacent planes they are aligned antiparallel. This results in a magnetic cell doubling and the emergence of purely magnetic peaks below the Néel temperature.

The NiO NPs were made using a pilot scale continuous hydrothermal flow synthesis process; a 20× volumetric scale up of an analogous laboratory process.[21] A complete description of the process, construction, and validation is presented elsewhere.[21–23] A schematic of the process used in this work is presented in Figure 1. Briefly, the NiO particles were produced by reacting a supercritical water flow issuing from P-1 at 450 °C, 24.1 MPa (350 ml min^{-1}) with a ambient temperature flow of 0.08M nickel (II) nitrate solution (P-2) combined with a flow of 0.1M KOH solution (P-3) each at 175 ml min^{-1} in a confined jet mixer (CJM), the temperature of the mixture was 335 °C. Upon mixing the supercritical water with the precursor solutions, the rapid hydrolysis and dehydration of the Ni salt lead to the formation of many particle nucleates with minimal growth. After formation in the CJM, the particles were cooled in flow and were collected as slurry at the end of the process after passing through a back pressure regulator used to maintain the process at 24.1 MPa. The slurry containing the NP was cleaned by dialysis against a buffer solution of >15 MΩ deionized (DI) water. After dialysis, NiO was freeze-dried. The particles were left intentionally uncoated in order to minimise the incoherent scattering due to hydrogen, which would otherwise occur in a neutron experiment.

A detailed structural determination was carried out using the high resolution neutron powder diffractometer, D2B, at the Institut Laue-Langevin (ILL) in Grenoble. Since the coherent nuclear scattering amplitudes of the constituent elements in this study, Ni (10.3 fm) and O (5.803 fm), are significantly different, neutron diffraction is particularly appropriate. Using D2B and a neutron wavelength of 1.59 Å, diffraction patterns were recorded over the two-theta range 10° to 150° in steps of 0.05°. The sample was placed in a thin walled vanadium can of diameter 5 mm, which was located in an "orange ILL cryofour" providing stable temperatures of 5 K and 550 K. The diffractometer was calibrated and the intrinsic resolution was determined using a "standard" powder sample of alpha $Na_2Ca_3Al_2F_{14}$, the resolution, so determined, was then used in the refinement of the NiO data. Due to the finite size of the particles, the lattice diffraction peaks were broadened commensurate with the particle size. Using the Scherrer peak broadening formula, it is hence possible to extract the sizes of the overall lattice producing the broadening. This can be done either manually by fitting each peak with an individual Gaussian, or using refinement programs such as "Fullprof." The peaks of the NiO NP were typically a factor of 6.2 wider compared to the standard sample, showing this is not a small effect.

The refinement was carried out using the "Fullprof" profile fitting suite and analysis of the individual peaks was achieved using both "Fullprof" and also by convoluting a Gaussian response with the observed profile of the standard sample at the same or approximately the same two theta value for comparison. This was done due to the small number of magnetic peaks, which were observed. Both of these approaches were found to give very similar results.

SQUID magnetometry was carried out using a Quantum Design MPMS over a range of temperatures (400–5 K) measuring hysteresis loops and magnetisation as a function of temperature, time, and applied field. These measurements were taken for both NiO nanoparticles as well as NiO powder as a reference sample consisting of particles many microns in size, obtained from Sigma-Aldrich, in order to determine the bulk behaviour.

RESULTS

The nanoparticles were confirmed as free from possible nitrates by thermo-gravimetric analysis (not shown). X-ray powder diffraction was also used to check their pure stoichiometry and to estimate the structural size. Transmission electron microscopy was performed to check their crystallinity and monodispersity, as shown in Figure 2.

The neutron powder diffraction patterns, taken at 550 K and 5 K, are shown in Figure 3. The fitted profile (black) and difference between the fit and the data is inset, indicating an excellent match, the chi squared values for the 550 K and 5 K fit are 2.5 and 2.9, respectively. The peak at around

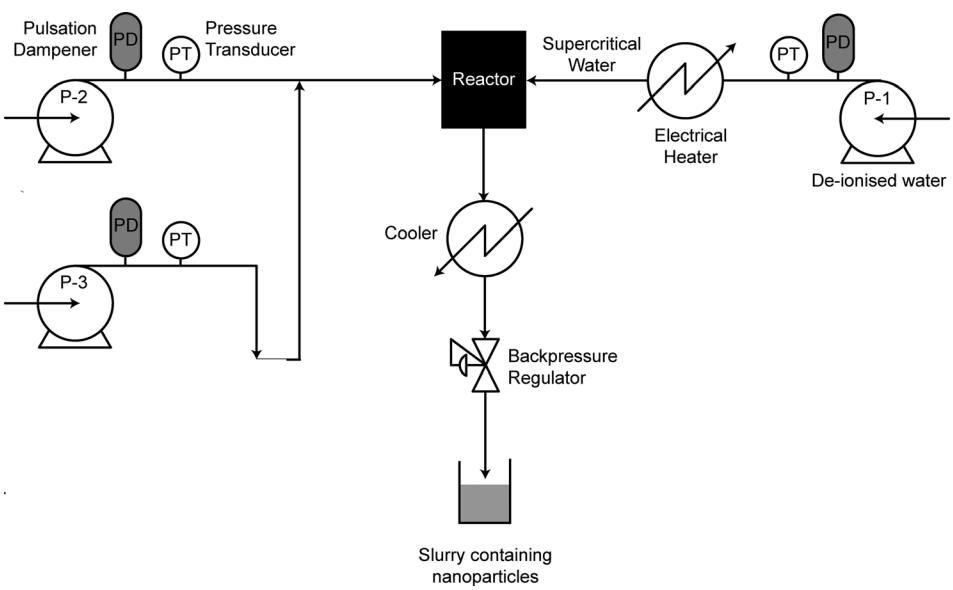

FIG. 1. A schematic of the NP synthesis method. Supercritical water from P-1 is mixed with ambient nickel nitrate from P-2 and potassium hydroxide from P-3 in a confined jet mixer. This precipitates out the nanoparticles, which are collected from the slurry after cooling.

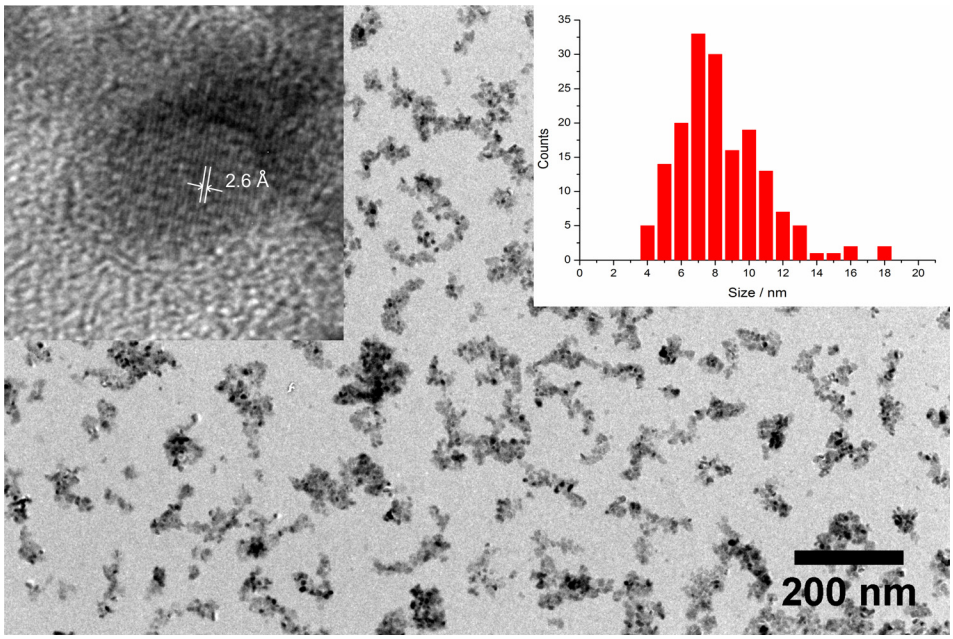

FIG. 2. Transmission electron micrograph of the NiO particles showing their relative monodispersity (size histogram inset right gives an estimate of 7(2) nm) and the inset left demonstrates their crystallinity.

$2\theta = 40°$ is due to the cryostat as was confirmed by removing the sample and measuring again. At high angles, both the patterns are very similar (due to the decay of the magnetic form factor);[24] however, at low angles new peaks emerge due to the onset of antiferromagnetism below T_N. The peak near 13° has been indexed as the ($^1/_2$ $^1/_2$ $^1/_2$) reflection and is the focus of our study of the magnetism in NiO NP. Refinement of the magnetic structure using all the magnetic peaks leads to a solution identical to that of bulk NiO found by Roth,[25] i.e., a type 2 antiferromagnet with a moment of $1.90 \pm 0.02\ \mu_B$ per nickel atom directed along the [1 1 –2] direction, perpendicular to the projection vector.

Several peaks were used to determine any lattice contractions due to thermal expansion or other effects which may occur with temperature. Due to the enhanced peak widths, it was not possible to identify any splitting arising from magnetostrictive transitions below T_N.[26] For the (2 2 0) nuclear peak, this is shown in Figure 4. Superimposing the (2 2 0) profiles observed at 5 K and 550 K shows that the peak shape does not change over this temperature range, indicating the stability of the particle size and shape.[26] Comparing the diffraction pattern with that from a standard ($Na_2Ca_3Al_2F_{14}$) clearly shows that the Bragg peaks of the NiO NP are significantly broadened. A systematic comparison shows that the broadening is uniform and consistent with the presence of spherical particles. However, at 5 K a slight lowering of the background is visible due to decreased thermal scattering at low temperature, though the full width at half maximum is unaffected. Therefore, no temperature dependant corrections were needed to the structure in the microstructural analysis.

Whilst all the peaks were used to refine the magnetic and structural core sizes in the microstructural analysis, the ($^1/_2$ $^1/_2$ $^1/_2$) and the (2 2 0) were the clearest purely magnetic and structural peaks, respectively. The fits to these peaks are shown in Figure 5 and the results are presented in Table I.

The particle size is consistent with the TEM images, inset Figure 2, which estimate the size as 70(15) Å; however,

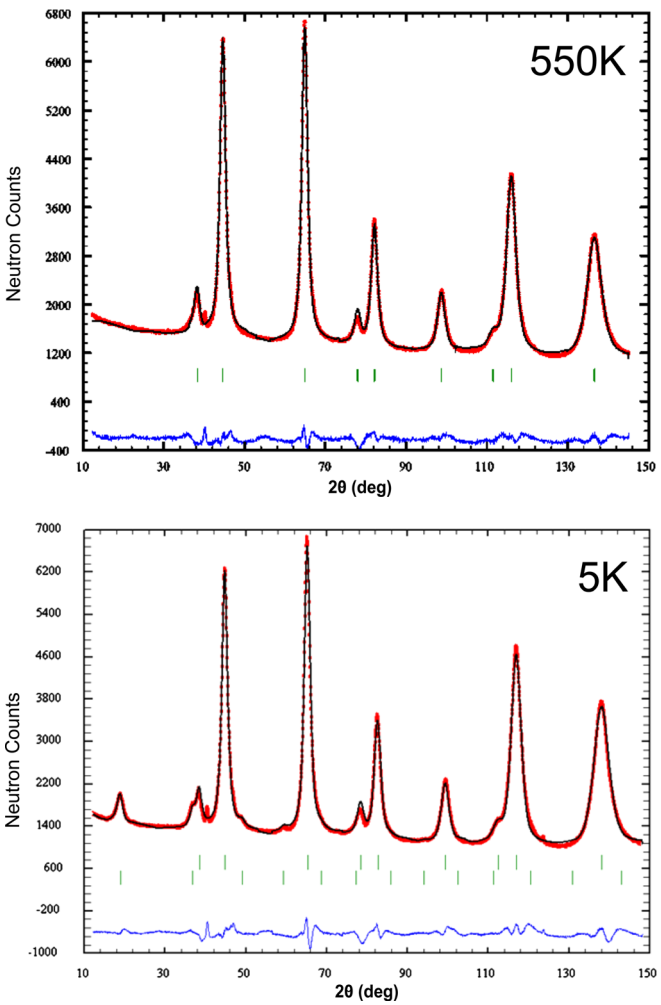

FIG. 3. Neutron powder diffraction (red) and fit (black) for the NiO NP at 550 K (top) and 5 K (bottom). The peak around 40° arises from the cryostat; at low temperatures, below T_N, an additional peak arises due to the antiferromagnetic ordering of the NiO, clearly visible near 13°. The bottom line (blue) is the difference between the data and the fit; the 550 K and 5 K datasets have χ^2 values of 2.5 and 2.9, respectively.

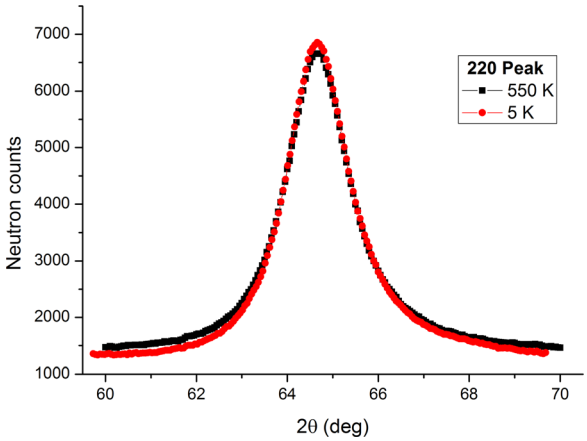

FIG. 4. A view of the (220) structural peak at both 550 K and 5 K showing the FWHM, which is temperature invariant.

the antiferromagnetic core differs from the size of the NP. These results provide proof that the surface layer of the NP possess no spontaneous long range order and that this layer is around 7 Å thick. We now continue our investigation using SQUID magnetometry in order to determine the nature of this layer.

Isotherms were measured at temperatures ranging from 5 K to 400 K and selected traces are shown in Figure 6 with an inset of magnetisation measured as a function of temperature. Large NiO crystals were measured over the same field and temperature ranges and confirm that the magnetic signal from the MNP originates from the magnetism of the outer shell, rather than the antiferromagnetic core. The isotherms at 100 K, 200 K, and 300 K have a curvature similar to that observed in superparamagnets or para/antiferromagnets with a polarisable impurity. However, neither of these scenarios seems applicable. As we can see in the inset of Figure 7, the Langevin function provides a poor fit to the normalised data at 325 K and lowering the temperature only deteriorates the fit, so they do not behave superparamagnetically. The temperature dependence of the curves is shown in the main part of Figure 7. The nature of the system means that the polarisable impurity seems implausible also. Instead, we predict a frustrated, disordered spin arrangement with competing interactions between the antiferromagnetic bulk coupling, the surface shape anisotropy, and the applied magnetic field. In this case, the first two anisotropies will be local environment dependant.

Below 30 K, there is a transition to an additional state with higher magnetic anisotropy. This is indicated by the 10 K and 5 K (not shown) isotherms having a smaller initial gradient and crossing over the higher isotherms and also by the reduction in magnetisation in the magnetisation versus temperature measurements. The correlations giving rise to the curvature in the isotherms have gone by 375–400 K

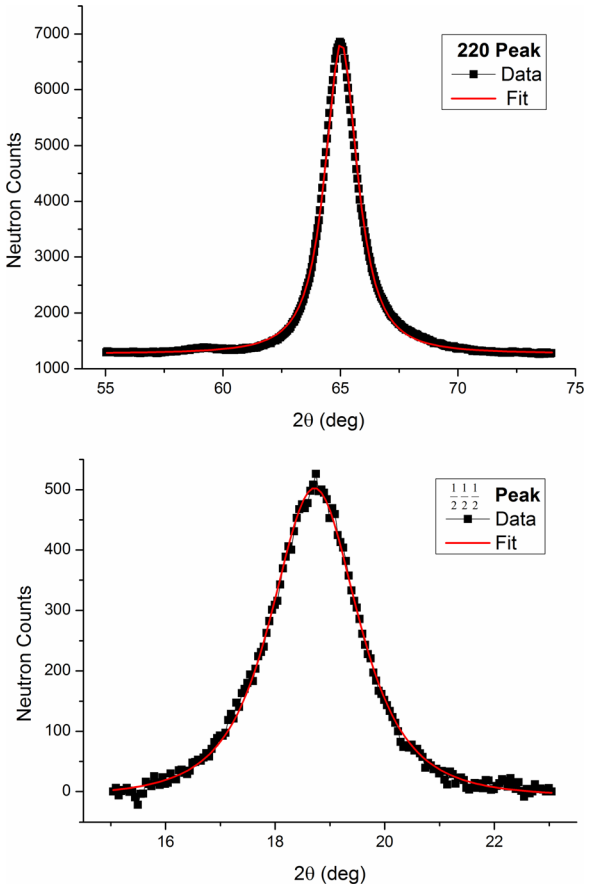

FIG. 5. The structural (2 2 0) peak at 550 K and the magnetic (½ ½ ½) peak at 5 K with Gaussian fit convoluted with the instrument resolution function used to determine the particle size.

indicating a broad transition around 350 K. The same responses are not visible in isotherms taken on the large NiO reference crystals, thus it must be a surface effect.

The 400 K isotherm is essentially linear with a susceptibility of $\sim 27 \times 10^{-5}$ emu g^{-1}, which is approximately 3 times larger than that of antiferromagnetic bulk NiO at the same temperature.[27] This we attribute to being below the transition temperature of the apparent onset of "ferromagnetism" due to polarisable, non-antiferromagnetically aligned spins in the shell.

A series of magnetisation measurements were taken with time at various temperatures, the NPs were cooled in a field (10 000 Oe data shown) which was then removed, the resulting relaxation of magnetisation with time was measured. It was found that the NP relaxed at temperatures up to 300 K (the highest measured), but the magnitude of the moment was reduced with temperature. The decay of the magnetisation was fitted using a simple exponential decay of the form

$$M = M_0 e^{-\frac{t}{\tau}} + M_\infty. \quad (1)$$

TABLE I. A summary of the results of fitting the nuclear and magnetic peaks to find their relative sizes.

	TEM diameter [Å]	Diameter [Å]	Volume [$\times 10^{-20}$ cm^3]	Mass [$\times 10^{-19}$ g]	N_{Ni} [atoms]
Particle	70(20)	65(1)	14.3	9.6	7890
Core	…	51(1)	6.95	4.63	3810

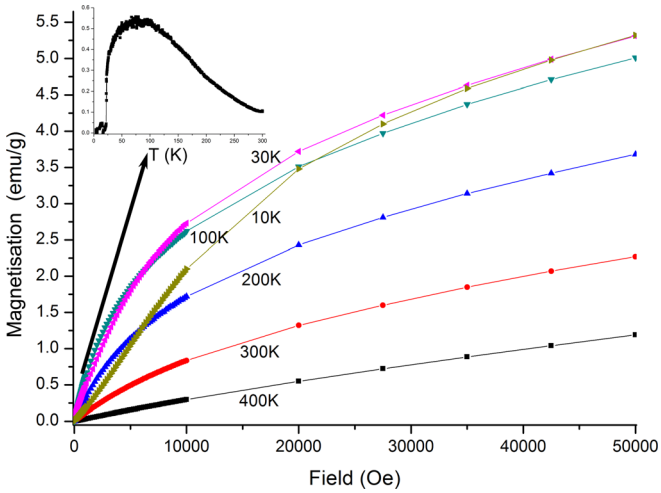

FIG. 6. Selected isotherms of NiO nanoparticles showing the transition from mostly paramagnetic at 400 K to a form of superparamagnetism from 200 to 30 K then finally to a state of higher magnetic anisotropy below 10 K. Inset shows magnetisation versus temperature in an applied field of 1000 Oe showing clearly the same transitions.

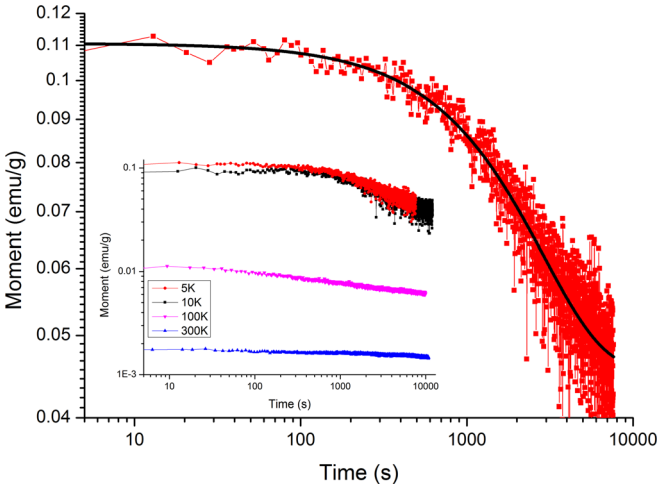

FIG. 8. Magnetisation versus time measurements, the main graph shows the magnetisation relaxation as a function of time at 5 K for NP cooled in a field of 1 T, which was then removed. The black line through the data is a simple exponential decay fitted to the data. Inset shows the same measurements made at different temperatures, all showing the same exponential relaxation of the magnetisation.

The time constant τ varied with temperature and the constants M_0 and M_∞ are the magnetisations at zero and infinite times, respectively. The fit of the relaxation to a simple exponential decay rather than a stretched exponential or a logarithmic dependence is in contrast to previous experiments on spin glasses.[28,29] A simple exponential is equivalent to a stretched exponential with zero stretching factor, but based on the theory behind their stretching factor,[30] which would require an unphysical infinite dimensional potential trapping the spins. Thus, we can rule out a traditional spin glass as the magnetic structure in the shell of the particles

Hysteresis loops of the particles were taken at 5 K, having previously been cooled from 400 K both with and without a field of 50 000 Oe as shown in Figure 8. The field cooled (FC) and zero field cooled (ZFC) loops are shown in Figure 9. The coercivities of both loops are 410(10) Oe with the steps at 1700(100) Oe. The remnant field for the ZFC is 1.10(2) emu/g, whereas for the FC case it is higher, at 1.56(2) emu/g and the steps in magnetisation are 1.00(2) emu/g and 1.21(2) emu/g, respectively. It can be seen that there is no exchange bias effect, nor any change in the coercivity as has been previously reported.[31,32] However, the theory of traditional exchange bias is not necessarily applicable in the case of antiferromagnetic cores with disordered outer shells, which can be ferromagnetically aligned.

Instead there is an increase in the moment of the particles for a given field. This may either be due to an enhancement of the low temperature high anisotropy state, for instance, competing cubic and uniaxial anisotropies,[33] or to our field cooling routine not being able to go to temperatures over the shell's Curie temperature. This would mean that the ZFC measurement may not be that of the true ZFC state leaving room for unseen exchange bias effects. The inset of Figure 9 indicates the existence of competing anisotropies. We conjecture that these arise from a form of surface

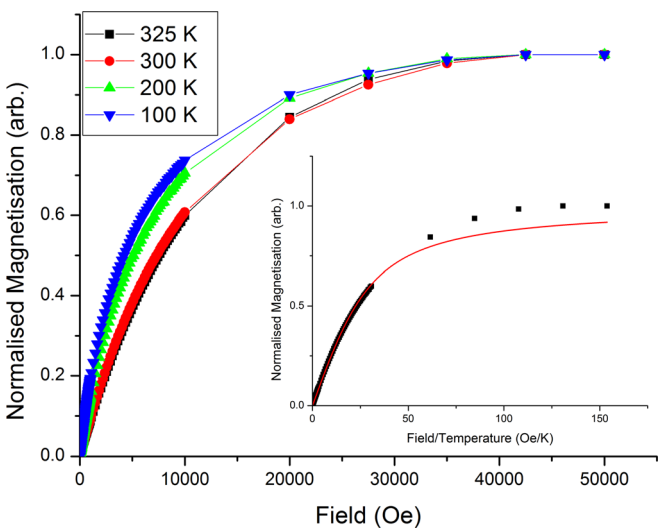

FIG. 7. Normalised isotherms with background paramagnetism removed, inset shows the 325 K curve fitted with a Langevin curve, showing poor agreement between superparamagnetic theory and these nanoparticles.

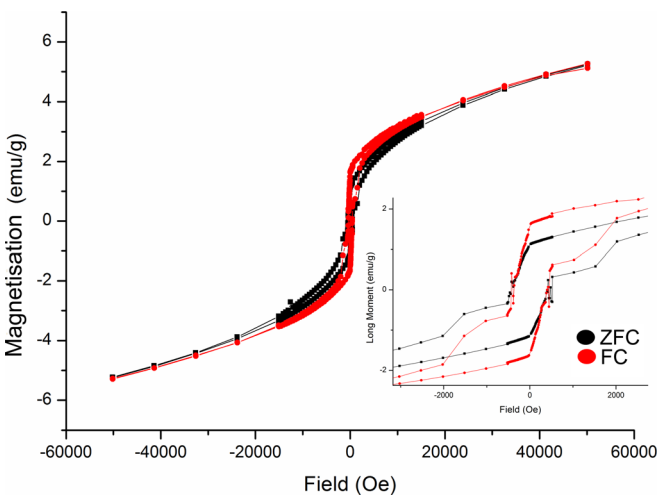

FIG. 9. Hysteresis loops taken at 5 K with field cooling (red) and zero field cooling (black) with zoomed inset.

induced shape anisotropy and exchange coupling from the core antiferromagnetically aligned spins. Further investigation using high temperature SQUID measurements are ongoing. All hysteresis loops and isotherms of the bulk NiO show purely paramagnetic behaviour, as expected.

DISCUSSION

As far back as Néel, it was realised that NiO is a good model system for antiferromagnetism, but that in fine grains (nanoparticles) some form of uncompensated magnetisation exists.[34] Our magnetisation results are of the same magnitude as Richardson[35] and Kodama.[32] However, the wide variations in published results imply that subtle differences in similarly made particles may produce relatively large variations in the apparent ferromagnetism. Kodama *et al.*, in particular, have published several papers on the origins of the magnetic moment[32,36,37] in NiO NP. For particles smaller than those in this study, they propose a number of discrete sublattices of non-collinear spins, whose presence is induced by the surface anisotropy with additional effects from the surface spins. Using neutron diffraction, these sublattices are indistinguishable from each other as they all lie in the plane perpendicular to the propagation vector. Though for the particle size investigated only two are expected from their calculations.[36] They also calculate[32] that the observed moments for NiO NP are too large for a simple type 2 antiferromagnetic lattice with uncompensated spins on the surface. Our results agree and are consistent with this, though their calculated and measured hysteresis curves have a markedly different shape from Figure 9.

The high resolution TEM images show that the lattice fringes seem to extend to the edge of the NP. Any defects of vacancies on the surface would be difficult to see in such images unless they were highly concentrated leading to disorder. Thus, it is impossible to rule out surface defects as the cause of the effects mentioned here; however, it is unlikely that such vacancies would extend all the way to the core in every particle and cause the magnetic effects seen here. It is also unlikely that the structural neutron diffraction peaks are all fitted with very little strain and no additional surface layer. Thus, we rule out such an explanation for the effects seen here.

By proving the existence of the non-antiferromagnetic shell of spins, we can see that averaging over the entire particle is not appropriate to characterise them. Instead, the magnetisation per gram of active material should be used, which is a factor of almost two in this case, giving approximately 10 emu g^{-1} at low temperatures. This is around a fifth of the saturation magnetisation of pure nickel[38] (55 emu g^{-1}), implying a much less disordered surface state than previously reported.[32,39]

Wismayer *et al.*[40] used polarised small angle neutron scattering (PSANS) to look at granular, ferromagnetic, thin films. They found very similar results to those presented here. Their grains were of a similar size (6 nm) and tantamount to MNP (they modelled them as such) and they found a similar result with a shell of 13.5 Å around the ferromagnetic core. We hypothesise that the thickness of the disordered shell will be a function of the size of the nanoparticle (the radius of curvature at the surface) as well as the exchange stiffness of the material.

Several papers[41,42] have explored the effects of dipole-dipole interactions in magnetic NP systems. Jonsson *et al.*[41] found that the effects of dipole-dipole interactions on ferromagnetic particles caused longer relaxation times than would be expected for non-interacting particles at low temperatures and that above some temperature (45 K in their case) that the relaxation was best described by single particle dynamics. Vargas *et al.*[42] found that the interactions could be accounted for with an additional (fictitious) temperature added to the denominator of the Langevin function, which acts to increase the blocking temperature of their system with increasing dipolar interaction strength. In such systems, it is reasonable to assume simple, single domain particles which can then form complicated magnetic arrangements where each particle is effectively a macro-spin. In the case of a polarizable outer shell of nominally antiferromagnetically aligned spins, this picture will not hold. It is possible, even probable, that the particles can then interact in some manner and arrange themselves into a magnetically stable state. However, the outer surfaces of these NP are also likely to do this, on an atomic scale. Quantitatively separating the two effects would be extremely difficult, but we can make some observations. Kodama *et al.*[43] estimate that the dipolar field from $NiFe_2O_4$ particles is <200 Oe; based on this estimate, all high field (>1000 Oe) measurements should correspond to the individual particle behaviour. Below this, we would expect only a small perturbation on the single particle behaviour, which may correspond to a different effective temperature. It is expected that these interactions will be most important in the 0–200 Oe regime, which is mostly unimportant for this study. Further investigations, separating the dipolar effects, could be carried out by dispersing various concentrations of NP in paraffin.

CONCLUSIONS

We have shown conclusive proof of the core/shell model of magnetism in antiferromagnetic NiO nanoparticles and ruled out surface defects/vacancies as the cause of such. The core of the particles is antiferromagnetic as expected; however, the shell exhibits an unexpectedly large permanent moment. Magnetic measurements show that there are two magnetic transitions between 400 and 10 K, a broad transition from paramagnetic to a form of superparamagnetism around 350 K and to a state of higher magnetic anisotropy at around 30 K. This state is confirmed by the difference in magnetisation between field cooled and zero field cooled hysteresis loops at 5 K. However, these loops show no evidence of exchange bias effects.

ACKNOWLEDGMENTS

The authors would like to thank the EPSRC and Cambridge Philosophical Society for funding and J. R. Cooper for assistance with the thermogravimetric measurements. Nguyen T. K. Thanh thanks the Royal Society for her university research fellowship. A.I. would like to thank Dr. D. D. O'Regan (EPFL) for useful discussions on NiO NPs.

[1]C. Gill, B. Price, and C. Jones, J. Catal. **251**, 145 (2007).
[2]P. D. Stevens, J. Fan, H. M. R. Gardimalla, M. Yen, and Y. Gao, Org. Lett. **7**, 2085 (2005).
[3]R. Rungsawang, J. da Silva, C.-P. Wu, E. Sivaniah, A. Ionescu, C. Barnes, and N. Darton, Phys. Rev. Lett. **104**, 255703 (2010).
[4]D. Pouliquen, R. Perdrisot, A. Ermias, S. Akoka, P. Jallet, and J. Le Jeune, Magn. Reson. Imaging **7**, 619 (1989).
[5]J. Llandro, J. J. Palfreyman, A. Ionescu, and C. H. W. Barnes, Med. Biol. Eng. Comput. **48**, 977 (2010).
[6]N. T. K. Thanh, *Magnetic Nanoparticles: From Fabrication to Clinical Applications* (Taylor and Francis, 2012), p. 584.
[7]Q. A. Pankhurst, N. K. T. Thanh, S. K. Jones, and J. Dobson, J. Phys. D: Appl. Phys. **42**, 224001 (2009).
[8]O. Veiseh, J. W. Gunn, and M. Zhang, Adv. Drug Delivery Rev. **62**, 284 (2010).
[9]N. J. Darton, A. J. Sederman, A. Ionescu, C. Ducati, R. C. Darton, L. F. Gladden, and N. K. H. Slater, Nanotechnology **19**, 395102 (2008).
[10]C. Haase and U. Nowak, Phys. Rev. B **85**, 045435 (2012).
[11]E. Kita, T. Oda, T. Kayano, and S. Sato, J. Phys. D: Appl. Phys. **43**, 474011 (2010).
[12]S. M. Morgan and R. H. Victora, Appl. Phys. Lett. **97**, 093705 (2010).
[13]Y. Labaye, O. Crisan, L. Berger, J. M. Greneche, and J. M. D. Coey, J. Appl. Phys. **91**, 8715 (2002).
[14]O. Iglesias and A. Labarta, Phys. Rev. B **63**, 184416 (2001).
[15]R. N. Bhowmik and R. Ranganathan, Solid State Commun. **141**, 365 (2007).
[16]R. Bhowmik, R. Nagarajan, and R. Ranganathan, Phys. Rev. B **69**, 054430 (2004).
[17]M. Tadic, M. Panjan, D. Markovic, B. Stanojevic, D. Jovanovic, I. Milosevic, and V. Spasojevic, J. Alloys Compd. published online, doi: 10.1016/j.jallcom.2012.10.166.
[18]M. A. Khadar, V. Biju, and A. Inoue, Mater. Res. Bull. **38**, 1341 (2003).
[19]S. Mandal, S. Banerjee, and K. S. R. Menon, Phys. Rev. B **80**, 214420 (2009).
[20]M. Eisenberg and R. Guy, Am. Math. Monthly **86**, 571 (1979).
[21]C. J. Tighe, R. Q. Cabrera, R. I. Gruar, and J. A. Darr, Ind. Eng. Chem. Res. **52**, 5522 (2013).
[22]C. Y. Ma, C. J. Tighe, R. I. Gruar, T. Mahmud, J. A. Darr, and X. Z. Wang, J. Supercrit. Fluids **57**, 236 (2011).
[23]C. Y. Ma, X. Z. Wang, C. J. Tighe, R. Gruar, and J. A. Darr, Trans. Am. Inst. Chem. Eng: Advanced Control of Chemical Processes **8**, 874 (2012).
[24]L. Dobrzynski and K. Blinowski, *Neutrons and Solid State Physics* (Ellis Horwood Limited, 1994).
[25]W. Roth, Phys. Rev. **110**, 1333 (1958).
[26]N. Tombs and H. Rooksby, Nature **165**, 442 (1950).
[27]J. Singer, Phys. Rev. **104**, 929 (1956).
[28]S. Tiwari and K. Rajeev, Phys. Rev. B **72**, 104433 (2005).
[29]R. Chamberlin, G. Mozurkewich, and R. Orbach, Phys. Rev. Lett. **52**, 867 (1984).
[30]P. Grassberger, J. Chem. Phys. **77**, 6281 (1982).
[31]S. A. Makhlouf, F. T. Parker, F. E. Spada, and A. E. Berkowitz, J. Appl. Phys. **81**, 5561 (1997).
[32]R. Kodama, S. Makhlouf, and A. A. Berkowitz, Phys. Rev. Lett. **79**, 1393 (1997).
[33]M. Gester, C. Daboo, R. J. Hicken, S. J. Gray, A. Ercole, and J. A. C. Bland, J. Appl. Phys. **80**, 347 (1996).
[34]L. Neél, in *Low Temperature Physics*, edited by C. DeWitt, B. Dreyfus, and P. G. De Gennes (Gordon and Breach, 1961), p. 413.
[35]J. T. Richardson, D. I. Yiagas, B. Turk, K. Forster, and M. V. Twigg, J. Appl. Phys. **70**, 6977 (1991).
[36]R. H. Kodama, J. Magn. Magn. Mater. **200**, 359 (1999).
[37]A. E. Berkowitz, R. H. Kodama, S. A. Makhlouf, F. T. Parker, F. E. Spada, E. J. McNiff, Jr., and S. Foner, J. Magn. Magn. Mater. **196–197**, 591 (1999).
[38]J.-H. Hwang, V. P. Dravid, M. H. Teng, J. J. Host, B. R. Elliott, D. L. Johnson, and T. O. Mason, J. Mater. Res. **12**, 1076 (1997).
[39]S. D. Tiwari and K. P. Rajeev, Thin Solid Films **505**, 113 (2006).
[40]M. P. Wismayer, S. L. Lee, T. Thompson, F. Y. Ogrin, C. D. Dewhurst, S. M. Weekes, and R. Cubitt, J. Appl. Phys. **99**, 08E707 (2006).
[41]T. Jonsson, P. Nordblad, and P. Svedlindh, Phys. Rev. B **57**, 497 (1998).
[42]J. Vargas, W. Nunes, L. Socolovsky, M. Knobel, and D. Zanchet, Phys. Rev. B **72**, 184428 (2005).
[43]R. Kodama, A. A. Berkowitz, J. McNiff, S. Foner, and E. McNiff, Phys. Rev. Lett. **77**, 394 (1996).